A case study on the use of infrared thermography to assess seepage zones in mining operations

by M. Maoyi[1], J.L. van Rooy[1], A. Lotriet[2], R. Bush[3], M.A. Dippenaar[1]

Affiliation:
1 Engineering Geology, Department of Geology, University of Pretoria, South Africa
2 Yellow Technical Services (Pty) Ltd, Johannesburg, South Africa
3 SRK Consulting (Pty) Ltd, Johannesburg, South Africa

Correspondence to:
M. Maoyi

Email:
mampho.maoyi@up.ac.za

Dates:
Received: 26 May. 2025
Revised: 01 Dec. 2025
Accepted: 06 Jun. 2026
Published: Aug. 2026

How to cite:
M. Maoyi, van Rooy J.L., Lotriet A., Bush R., Dippenaar M.A. 2026. A case study on the use of infrared thermography to assess seepage zones in mining operations. *Journal of the Southern African Institute of Mining and Metallurgy*, vol. 126, no. 8, pp. 435 – 446

DOI ID:
https://doi.org/10.17159/2411-9717/3739/2026

ORCiD:
M. Maoyi
https://orcid.org/0000-0003-0737-6548
J.L. van Rooy
https://orcid.org/0000-0003-4708-6991
M.A. Dippenaar
https://orcid.org/0000-0002-6807-1353

Abstract

Effective management of unsaturated fluid flow in open-pit excavations is critical, as mining disturbances like blasting can enhance fracture connectivity, permeability, and water infiltration, thereby compromising slope stability. Thus, this study evaluates infrared thermography as a non-invasive tool for detecting seepage zones in a fractured rock highwall at an open-pit quarry in South Africa. Additionally, field-scale measurements as well as photogrammetry data, are used to gain a better understanding of unsaturated flow behaviour in fractured rock masses. Based on the results of this study, passive infrared thermography established baseline thermal anomalies associated with natural groundwater seepage, revealing distinct cooler surface patterns in highly fractured domains that aligned with geotechnical mapping. Active infrared thermography using controlled injection of cold water into the high wall, enabled real-time thermal monitoring revealing geotechnical domain thermal contrasts on the high wall, confirming preferential channelling along lithological contacts. This non-invasive technique provides valuable insights into the thermal response of highwalls, and highlights the role of fracture networks in controlling fluid movement within geotechnical domains. The findings demonstrate that infrared thermography is a powerful and reliable technique for remotely evaluating areas susceptible to seepage on high walls, based on thermal pattern variations that are imperceptible to the naked eye. This effectiveness as a remote rock monitoring tool for detecting seepage zones in fractured rock masses highlights infrared thermography as a promising strategy for improving hydrogeological risk assessment in mining operations.

Keywords

Unsaturated fracture flow, rock slopes, seepage zone, infrared thermography, photogrammetry

Introduction

Blasting activities in open-pit excavations compromise the structural integrity of jointed rock masses and actively alter their natural permeability (Li et al., 2024). As a result, blasting may increase the connectivity of fracture networks by enlarging existing fractures or creating new fractures, allowing groundwater and rainwater to infiltrate the fractures within the rock mass. For instance, the increased formation of these discontinuities due to blasting raises concerns regarding water flow behaviour and pore water pressures within the slope, which can have implications on slope stability and overall safety (Lu et al., 2024). The effects of blasting on rock mass permeability and groundwater dynamics vary considerably based on several interrelated factors, including the physical and mechanical properties of the rock mass, prevalence and nature of discontinuities, rock density, groundwater presence, type of explosives used, blast design, and intensity of stress waves produced during blasting (Silva et al., 2019; Kaveh Ahangaran et al., 2022; Xu et al., 2022). Collectively, these variables can induce changes in groundwater dynamics, potentially changing established flow patterns in geotechnical domains. The practical implication of these changes is that as mining progresses, it becomes imperative to continually update geotechnical models to reflect evolving rock mass conditions (Abdulai, Sharifzadeh, 2019; Yeh et al., 2021). Consequently, a thorough understanding of groundwater flow in fractured rock mass is essential, particularly in complex geological systems where discontinuities act as primary hydraulic pathways.

Previous studies have identified challenges in understanding the implications of excavations on rock mass behaviour, groundwater dynamics and flow patterns within these fractured systems (Li et al., 2014; Zhao et al., 2017). For example, Li et al. (2014) investigated groundwater trends in an open-pit mining area using a generalised large well method alongside a confined-unconfined flow model. Their study demonstrated the impacts of mining on local groundwater dynamics, which were crucial for environmental management. Similarly, Zhao et al. (2017) proposed a comprehensive methodology that integrated hydrological modelling with field data to assess the influence of open-pit mining on groundwater systems. Nonetheless, the accuracy of such models is often compromised by assumptions related to geological, hydrological, and hydraulic properties, where deviations from real-geological conditions can substantially affect the confidence interval of the data and reliability of the findings. Despite these advances, developing a representative model that accurately reflects fracture parameters still remains a challenge, as many parameters must be extrapolated or inferred due to the complex nature of geological and induced processes that create discontinuities of varying scales and orientations (Huang et al., 2019). These complexities result in fractured media exhibiting pronounced spatial variability and anisotropy, leading to intricate fracture networks. Therefore, effective rock mass characterisation must consider various influential factors that include lithology, structural features such as faults and discontinuities, and conditions such as fracture frequency and weathering (Zimmerman, Paluszny, 2023). These parameters play a crucial role in determining the rock mass ratings, which can be further categorised into distinct geotechnical domains for stability assessments within rock engineering and rock mechanics applications (Bieniawski, 1973; Barton et al.,1974; Bieniawski, 1989; Laubscher, 1990; Zhang et al., 2019).

For researchers and industry consultants, a thorough understanding of fluid movement is vital for assessing the connectivity of fractures, a key component in rock monitoring, especially amidst ongoing geological changes in mining environments (Li et al., 2024). Currently, a multifaceted approach is commonly employed to characterise fluid flow behaviours in fractured media. This encompasses aquifer characterisation, analysis of recharge areas, and monitoring of water levels in open pit environments (Liu et al., 2021). While these techniques yield valuable insights, there is often a predominance of reliance on quantitative values and assumptions regarding flow patterns in the absence of direct observations of flow path geometries within the rock mass. This limitation is particularly acute in unsaturated conditions, where an upscaling framework is needed to better address gaps in understanding fluid flow in fractured rock masses (Zhang et al., 2021). The primary challenge of managing unsaturated fluid flow within open-pit mining environments lies not merely in identifying major discontinuity sets with similar orientations, but this is also related to determining which of these sets are hydraulically active within a specific geotechnical domain. This is essential for mitigating issues related to rock stability, particularly in situations exacerbated by blasting and periods of heavy rainfall when water can flow through major discontinuity planes associated with potential slope failures. Therefore, developing a robust monitoring strategy is increasingly vital to reduce rock slope risks.

To address the aforementioned challenges, the use of infrared thermography offers a promising avenue in studying the identification of groundwater zones and regions susceptible to seepage in rock mass (Meola, 2012; Sass et al., 2023). This non-invasive imaging technique captures and processes thermal information through thermal images by detecting infrared radiation emitted by objects and converting the image into temperature values above absolute zero (Mineo, Pappalardo, 2021). For instance, Wu et al. (2005) assessed the integrity of rock masses in the context of shotcrete slopes, highlighting the technique's capability to identify eroded voids behind shotcrete applications. Similarly, Teza et al. (2012) utilised infrared thermography to remotely identify weaknesses in rock cliffs, showcasing its usefulness in characterising geotechnical properties by detecting features such as voids and material inhomogeneities. In a further step towards enhancing hazard detection, Gigli et al. (2014) proposed an integrated methodology that combines terrestrial laser scanning with terrestrial infrared thermography for monitoring stability and detecting instabilities on slopes. Their findings illustrate that thermal images collected during assessments can reveal unstable rock masses, highlighting the importance of employing advanced techniques in geological surveys to improve risk management. However, a notable gap exists in the literature surrounding the application of infrared thermography in hydrogeology, rock engineering, and rock mechanics.

According to the authors' knowledge, the work by Rosenbom and Jakobsen (2005) remains the only study linking infrared thermography with fracture analysis and groundwater flow in chalk formations in Denmark. Their experimental framework involved the injection of cold water into a fractured chalk high wall in a quarry, aimed at assessing hydraulic connectivity. However, the absence of a robust baseline and reliance on qualitative thermal image interpretation limited the study's conclusions. Thus, this study builds on the groundwork established by Rosenbom and Jakobsen (2005) and expands the application of infrared thermography to South African geological formations. Specifically, it focuses on the quartzitic sandstones of the Daspoort Formation of the Transvaal Supergroup. Field experiments involving passive monitoring under ambient conditions and active cold-water injection are conducted on an exposed quarry high wall. The resulting thermal imagery is analysed using complementary qualitative (visual anomaly detection) and quantitative (temperature differential) methods, with interpretations integrated against detailed geotechnical characterisation of the rock mass to elucidate seepage zones in fractured rock environments.

Aims and objectives

The aim of this study is to evaluate the effectiveness of infrared thermography as a non-invasive, remote monitoring tool for detecting seepage zones in fractured rock masses within mining operations. Through a field-based case study at a quarry site, the research seeks to demonstrate the technique's potential as a practical strategy for enhancing the understanding of unsaturated fluid flow behaviour in fractured rock environments.

The objectives of this study are as follows:

- Conduct passive and active infrared thermography (IRT) experiments on the quarry high wall to capture thermal signatures and anomalies indicative of unsaturated flow and seepage zones.
- Analyse thermographic data qualitatively and quantitatively to delineate areas susceptible to seepage.
- To integrate IRT findings with geotechnical characterisation of the high wall, assessing the overall effectiveness and limitations of IRT for non-invasive seepage detection in fractured rock.

Geological setting

This study was conducted at a quarry site in South Africa. The bedrock in this region forms part of the sedimentary rocks of the Daspoort Formation, Transvaal Supergroup (Figure 1). The open pit quarry lies in competent quartzitic sandstones of the late Archaean to early Proterozoic (2.65 – 2.05 Ga), with diabase sills and dykes intruding along weak discontinuities in the quartzitic sandstone (Eriksson et al., 2006). The later intrusion of the Bushveld Igneous Complex (2.05 Ga) resulted in contact metamorphism, producing quartzites from clastic protoliths (Eriksson, Reckzo, 1995). Weathering of the diabase occurs along the distinct contact zones directly above and below the sill. The Bushveld deformational event later affected the Transvaal Supergroup succession, which resulted in the development of folds and faults with a general northwest-southeast-to-north vergence (Eriksson et al., 2006).

The pit layout typically features high wall faces with an overall slope angle of 58°. Planar failure occurred at the contact between quartzite and diabase on the southwestern high wall of the quarry, as illustrated in Figure 2. During the quarrying process, the removal of overburden led to stress relief, causing the overlying quartzite to displace along the contact with the diabase. This displacement resulted in the formation of tension cracks at the crest of the open pit and intense rainfall during summer resulted in increased water ingress into the tension cracks. Due to the impermeable nature of the diabase, interflow occurred along the contact between the diabase and quartzite, ultimately appearing in the pit face. This probably caused a sudden rise in pore pressure and a corresponding decrease in effective stress, leading to a reduction in shear strength and the occurrence of localised planar slope failure.

Methodology

Study site - southwestern high wall

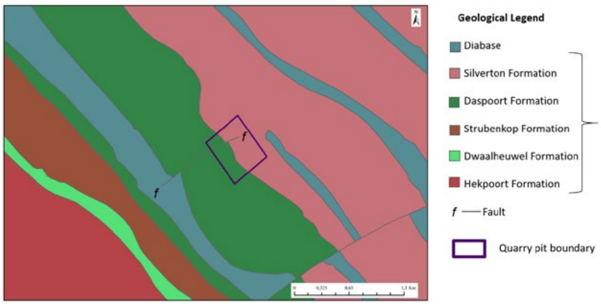

Figure 1—Geological map of the 2528 Pretoria Group Transvaal Supergroup, South Africa. Adapted from 1:250 000 Geological Map of 2528 Pretoria, 1978 (Council for Geoscience South Africa, 2020)

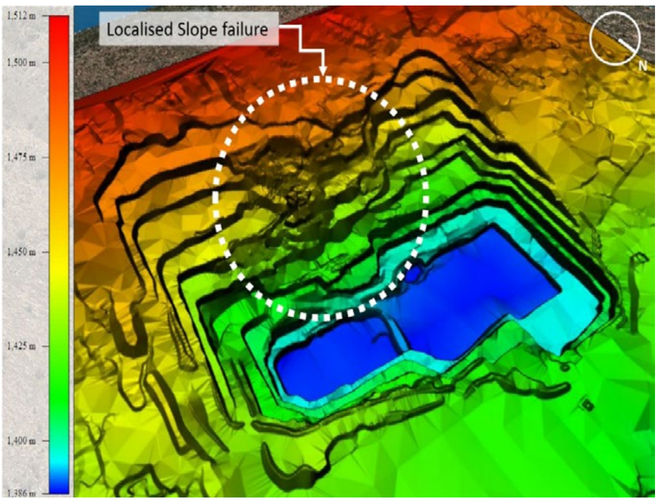

Figure 2—Digital terrain model of the quarry pit (~14 hectares)

The experimental site selected for infrared thermography monitoring is situated on the southwestern high wall of the open-pit mine, at the lowest accessible bench (Bench 1), where persistent groundwater seepage has been observed. This location was chosen due to the visible emergence of groundwater at the contact between highly weathered diabase and the quartzitic sandstone of the Daspoort Formation (Figure 3). The same section has previously experienced a localised slope failure, highlighting the significance of discontinuities in facilitating preferential flow pathways under both unsaturated and variably saturated conditions.

The selected Bench 1 extends laterally for approximately 60 m and has an average height of 10 m. Furthermore, a vertical uncased 18 m borehole was drilled approximately 3 m behind the high wall crest. It was positioned directly above the natural seepage zone and intersected the weathered diabase layer (refer to the cross-section, Figure 4). This borehole served as the primary injection point for controlled water flow tests, with the static water level measured at approximately 5 m below the collar. This section of the high wall was subdivided into two distinct geotechnical domains, designated as Domain A and Domain B, as illustrated in Figure 4. The chosen intermediate scale for the field test is optimal: sufficiently large to encompass spatial variability in seepage behaviour, yet compact enough to permit detailed, high-resolution monitoring using infrared thermography together with complementary field measurements.

Geotechnical mapping

Prior to the field experiments, an integrated site investigation was conducted to assess the geotechnical properties of the selected high wall. The characterisation combined field window mapping

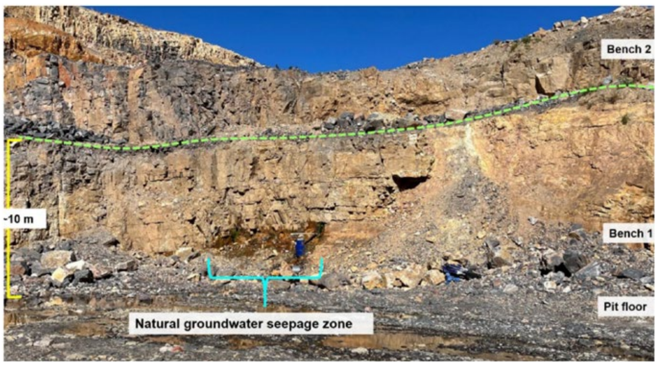

Figure 3—High wall study area (Bench 1) at ~1,400 m elevation for infrared seepage monitoring experiments

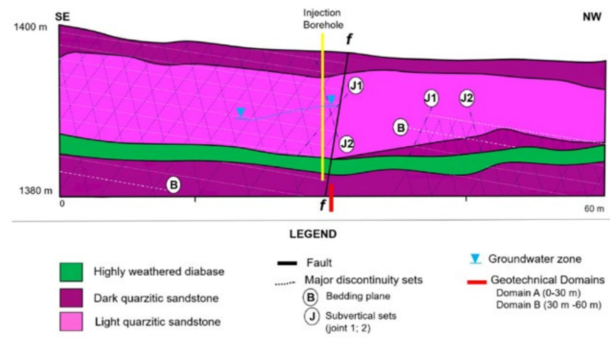

Figure 4—Geological cross-section of the southwestern high wall (Bench 1), showing geotechnical Domains A and B

with photogrammetry to improve the accuracy and detail of the geotechnical mapping. The mapping methodology followed the recommendations of the International Society for Rock Mechanics (ISRM, 1978), and further elaborated upon by Zangerl et al. (2022). This preliminary investigation provided the essential foundation for a detailed analysis of the lithological characteristics, structural features, and discontinuity orientations of the rock mass. Furthermore, key geotechnical features such as discontinuity sets and their persistence within the high wall, were also digitally extracted using Hive Map™ and 3GSM Shape Metrix™ (Rocscience®).

Thermal monitoring of the high wall

To identify areas on the southwestern high wall that could be susceptible to seepage and were not easily visible to the naked eye, surface temperature variations were monitored using the FLIR T1020® thermal camera. The camera was configured for time-lapse image acquisition, allowing continuous tracking of surface temperature distributions during experiments (Vollmer, Möllmann, 2018).

It is important to acknowledge that infrared thermography measurements are sensitive to several environmental and instrumental factors. This includes ambient conditions such as wind, precipitation, solar radiation, and camera calibration (Vollmer, Möllmann, 2018). These factors can introduce variability in surface temperature readings and affect measurement accuracy. Furthermore, accurate interpretation of thermal contrasts requires consideration of both meteorological conditions and the thermal properties of the rock mass, particularly surface emissivity and the presence of subsurface anomalies that may manifest as surface temperature differences. These parameters are critical, as they influence the transmission and detection of infrared radiation (Usamentiaga et al., 2014).

To minimise such effects, the camera was calibrated prior to data collection and experimental controls were implemented to improve the reliability of the temperature measurements (see Table 1). To complement infrared measurements and enable correction for atmospheric effects, ambient air temperature and relative humidity were continuously recorded using a pocket thermohygrometer.

Thermal images were acquired along the area of interest on Bench 1 of the southwestern high wall to ensure comprehensive spatial coverage, as depicted in the experimental setup (Figure 5). Both passive and active thermography techniques were employed to detect thermal anomalies associated with seepage zones by capturing emitted thermal radiation within the camera's field of view.

Passive thermography was conducted first to establish baseline surface temperature distributions under natural environmental conditions (Figure 5). This non-invasive technique relies on the detection of emitted thermal infrared radiation from the rock surface, which is directly related to its temperature (Vollmer, Möllmann, 2018). Thermal images were collected along the high wall to capture spatial variations in surface temperature for subsequent analysis.

To enhance detection sensitivity and delineate subsurface flow anomalies more effectively, active infrared thermography (IRT) was employed by applying a controlled thermal stimulus. Cold water (≈3 °C) was pumped into an uncased borehole to simulate seepage and induce a pronounced temperature contrast at the exposed rock surface relative to ambient conditions.

This setup included a water tanker as the cold-water source, fitted with a DN40 FlowVis® flow meter providing real-time flow rate monitoring, a non-return valve to prevent backflow, and a compatible discharge pipe for controlled delivery. The discharge pipe was inserted directly into the uncased injection borehole (Figure 5).

The field test started at 12:28 SAST by opening the control valve, pumping a total volume of 7000 L of water at a constant flow rate of 5 $m^3 h^{-1}$. Concurrent active IRT surveys monitored real-time surface temperature changes on the southwestern high wall until 14:00 SAST. This monitoring period permitted establishment of quasi-steady-state flow conditions in the fractured rock mass and development of a detectable thermal response at the exposed high wall face.

Post-processing of acquired thermal images

The captured thermal images were then transferred to FLIR Thermal Studio® for post-processing carried out in two steps. In the first step, qualitative analysis of the overall experimental data was performed, focusing on the visual observations of the entire high wall. This assessment utilised a colour-scaled palette thermogram, where each colour corresponds to a specific temperature measurement (Mineo et al., 2015). Therefore, target points were set within the thermograms, corresponding to temperature ranges based on the environmental conditions. This adjustment is necessary to accurately identify areas on the high wall that exhibited signs of moisture.

Following the qualitative assessment, the second step involved exporting the thermographic data for a more detailed quantitative analysis. Regions of interest (ROI) were defined to isolate geotechnical domains with differential surface temperatures. Temporal analysis tracked temperature changes throughout the acquisition sequence. Subsequently, minimum temperature values

Table 1

Transient field parameters

Parameters	
Emissivity	0.95
Ambient temperature	33 °C
Season in Southern Hemisphere	Autumn (April)
Camera distance from target point	~25 m
Camera resolution	1024x768
Camera lens	FOL21

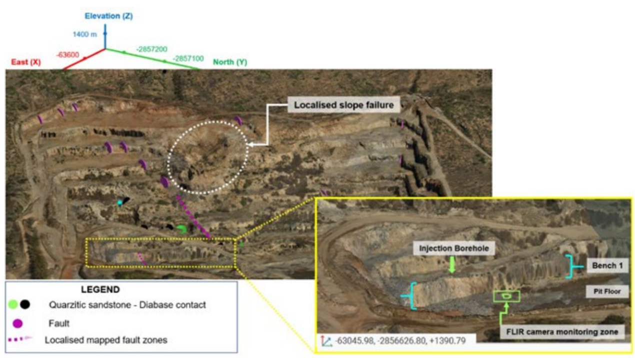

Figure 5—Experimental set-up

were extracted from each ROI to enhance detection of seepage-related thermal contrasts and improve anomaly identification. The final outputs were time-series temperature profiles for each ROI, focusing on key geotechnical subdomains. All processing parameters (e.g., emissivity, distance, palette) were kept constant to ensure comparability across datasets.

Results and analysis

Geotechnical domains within high wall

The high wall analysed in this study predominantly consists of quartzitic sandstones, which have been systematically classified into two distinct geotechnical domains.

Geotechnical Domain A (Figure 6a) features a 30 m wide window, primarily composed of slightly weathered, very hard quartzitic sandstone, which accounts for approximately 98% of the material. The remaining 2% is represented by weak, highly fractured soft rock, specifically weathered diabase, situated at the top of the slope. The photogrammetric model (Figure 6a) illustrates that this domain is characterised by rock mass exhibiting minimal discontinuities. Additionally, bedding planes and sub-vertical joints are prominent throughout the area, particularly within the lower 3 m of the pit. These discontinuities extend across a 20 m span but become less frequent in the upper 6 m of the high wall. Notably, within the remaining 10 m width of this geotechnical domain, no discontinuities were observed, and the groundwater conditions in the rock mass are reported to be dry.

Geotechnical Domain B comprises a 30 m wide window featuring a 9 m high bench, characterised by a pronounced blocky nature throughout the mapped area (Figure 6b). Blasting operations have markedly intensified this blockiness by artificially fracturing existing discontinuities within the rock mass. This domain consists of approximately 95% slightly weathered hard quartzitic sandstone and 5% weathered diabase. The weathered diabase layer, which is about 300 mm thick, runs parallel to the bedding plane of the quartzitic sandstone and is distinguished by a slightly undulating surface and a yellowish-brown colour, indicative of highly fractured medium to soft rock. Notably, this area is the only location in the pit where continuous groundwater flow with estimated flow rates of 9 L/s is observed, occurring at the contact between the weathered diabase and quartzite. This consistent flow leads to the saturation of the area, creating a natural groundwater seepage zone as shown in Figure 7.

A distinct transition occurs between Domain A and Domain B (Figure 8), marked by the minimal discontinuities of Domain A, which shift abruptly to the blocky characteristics of Domain B, delineated by a sub-vertical fault. Analysis of the 3D photogrammetric model confirmed that the discontinuity sets prevalent in Domain B do not persist to Domain A. Despite marked differences in fracture frequency, with Domain A showing much lower discontinuity density than the highly fractured Domain B, both domains are characterised by the same three major discontinuity sets. These comprise bedding planes and two sub-vertical joint sets (Table 2).

Initial insights from passive thermography

During passive thermography monitoring, the high wall at Bench 1 showed distinct thermal signatures. The ambient air temperature was recorded at 33 °C, whereas the rock surface temperature in both geotechnical Domains A and B reached approximately 56 °C. This thermal contrast is consistent with solar heating of the high wall, which absorbs visible and infrared radiation (Vollmer, Möllmann, 2018). However, the natural groundwater seepage zone in geotechnical Domain B has a cooler thermal signature of approximately 21 °C, clearly distinguishable from the warmer (56 °C) surrounding drier rock mass. (Figure 9). These observations

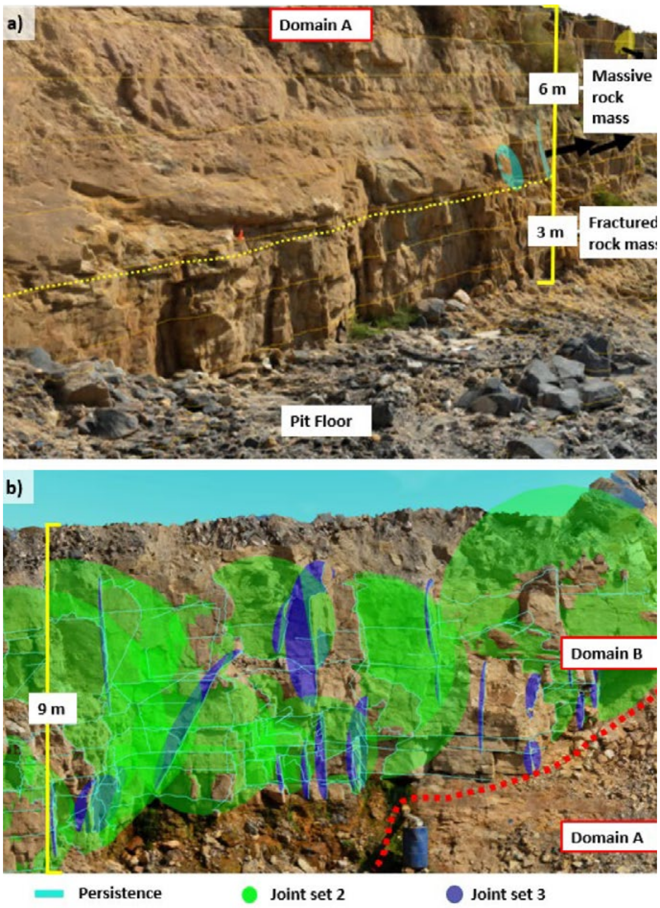

Figure 6—3D South western high wall photogrammetric model (a) geotechnical Domain A showing upper massive rock mass and bottom fractured rock mass - Shape Metrix™ (b) Domain B with the sub-vertical discontinuity sets and trace length for the persistence within the rock mass - Hive Map™

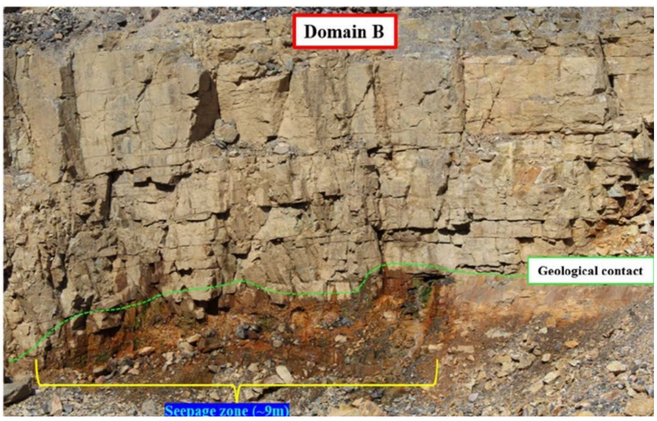

Figure 7—Geological contact between quartzitic sandstone (upper layer) and weathered diabase (lower layer), illustrating groundwater seepage zone

highlight the influence of environmental conditions on surface temperature distributions in open-pit high walls.

Active thermography for delineating seepage zones

During active thermography surveys of the high wall at Bench 1, introducing cold water (~3 °C) into a specific borehole acted as the main external thermal input to create measurable surface temperature differences. This controlled cooling resulted in distinct and spatially variable thermal anomalies across geotechnical Domain A and B.

In geotechnical Domain A (Figure 8), no detectable temperature contrasts or moisture related thermal signatures were observed during monitoring. Although the injection borehole was situated above the natural groundwater zone where downward or lateral spreading might be expected in this domain, the absence of cooling signatures suggests water migration was minimal or redirected. Moreover, the lack of thermal signatures in Domain A is likely due to its massive rock mass conditions and poorly developed hydraulic fracture network.

In contrast, spatially localised cooling was recorded along the exposed face in geotechnical Domain B, confirming rapid migration of the 3 °C injected water. To enable detailed analysis of the thermal response, Domain B was subdivided into two equal subdomains, B1 and B2. Each subdomain had a window width of 15 m and a bench height of 9 m (Figure 9). This subdivision facilitated closer examination of spatial variability in cooling patterns across the high wall.

Within Subdomain B1, qualitative thermal images did not reveal any additional thermal anomalies beyond the established natural groundwater temperature of approximately 21 °C (Figure 10). In contrast, quantitative time-series temperature measurements for this subdomain showed gradual declines and temporal fluctuations during the experiment (Figure 11). These quantitative trends indicate sustained migration of the cooler injected fluid within the high wall, even in the absence of prominent qualitative signatures.

Approximately 40 minutes into the field experiment, a new seepage zone emerged on the high wall face in Subdomain B2. Initially, no visible flow paths were present, and thermal contrast

Table 2

Discontinuity mapping data relating to major joint sets (average values)

Joint set	1	2	3	
Type	Bedding plane	Joint	Joint	Contact
Dip/dip direction	14°/040°	86°/322°	84°/054°	
Micro roughness	Rough undulating	Rough undulating	Smooth planar	Slickenside
Macro roughness	Straight	Slight undulation	Curved	
Infilling	Stained; sandy clay infill	Stained	Stained	Sandy silt
Alteration	Wall = rock	Wall = rock	Wall = rock	Wall < rock
Mean spacing	0.8 m	0.6 m	0.45 m	-
Aperture	3 mm	4 mm	2 mm	-
Minimum persistence	0.61 m	0.35	0.62	
Maximum persistence	16.34	6.41	3.66	> 20 m
Lithology	Quartzite	Quartzite	Quartzite	Quartzitic contact - highly weathered residual diabase

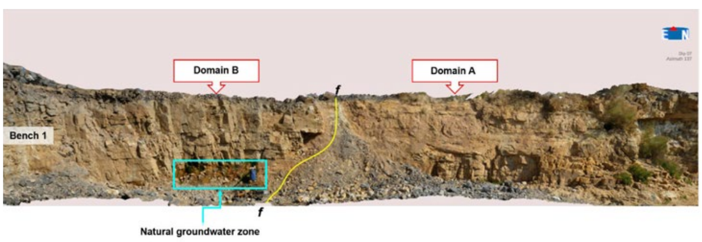

Figure 8—Photogrammetric model of Bench 1 illustrating the spatial transition from geotechnical Domain A to Domain B, delineated by a fault (Hive Map™).

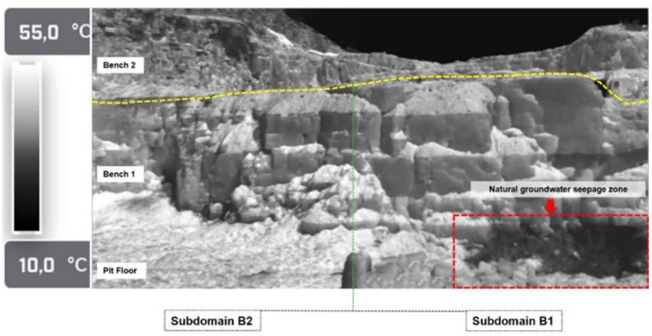

Figure 9—Thermogram of geotechnical Domain B before active thermography field experiment subdivided into Subdomain B1 and Subdomain B2

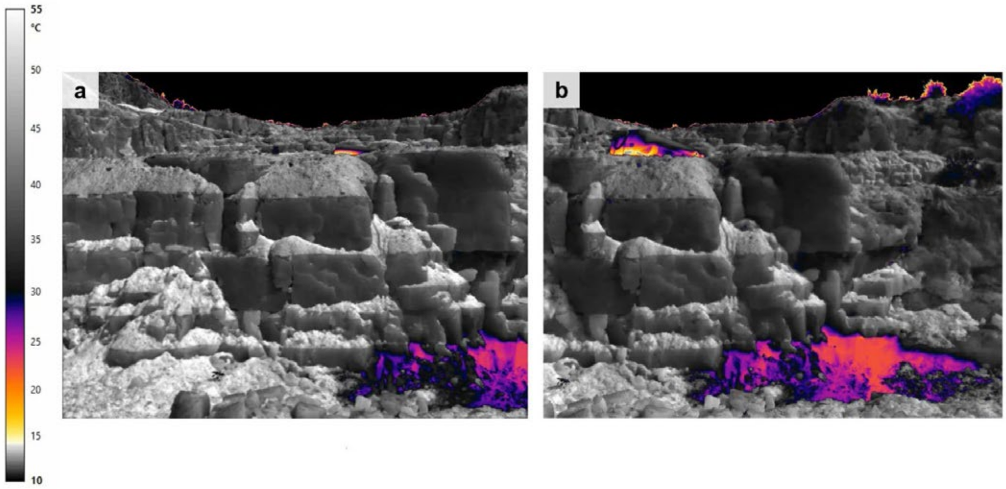

Figure 10—Thermograms of Subdomain B1 illustrating thermal characteristics at (a) the beginning and (b) the end of the experiment (with an adjusted viewing point for the subdomain)

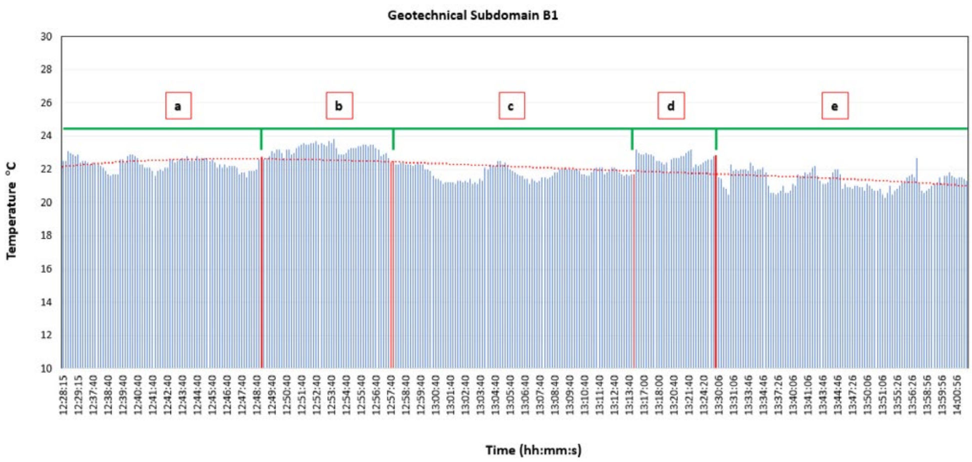

Figure 11—Subdomain B1 temperature versus time graph illustrating the temperature changes recorded at the beginning and end of the experiment

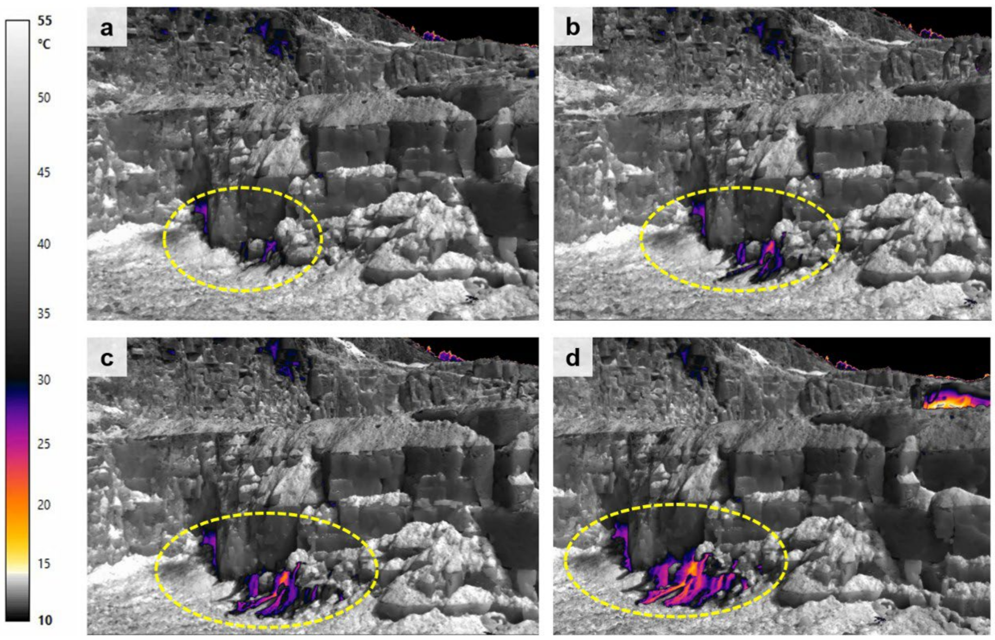

Figure 12—Thermograms of Subdomain B2 illustrating thermal characteristics at the beginning and conclusion of field test

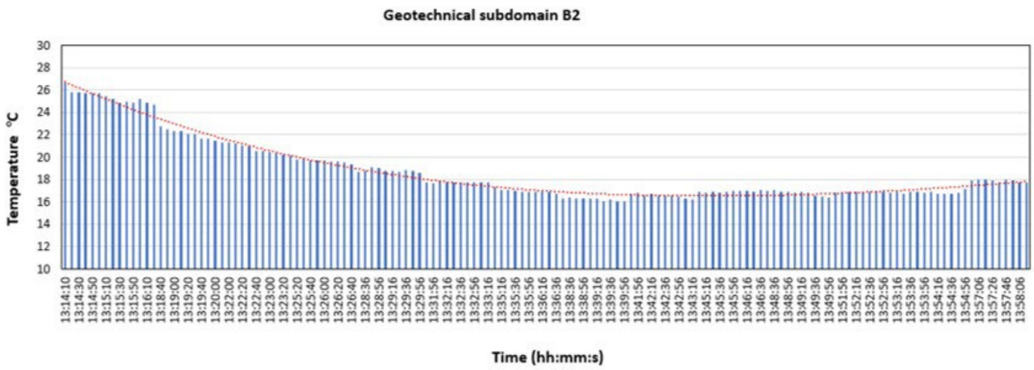

Figure 13—Subdomain B2 temperature versus time graph illustrating the temperature changes recorded at the beginning and end of the experiment

was minimal (Figure 12a). As the experiment continued, repeated wetting cycles during the injection test progressively expanded the wetting front on the rock surface, enabling the detection of subsurface flow through infrared radiation signatures (Figure 12b). The thermal images revealed the formation of new seepage zone governed by preferential flow paths that followed interconnected fracture networks and were oriented parallel or subparallel to bedding planes (Figures 12c – d). This new seepage outflow point coincided with the contact between quartzitic sandstone and weathered diabase, mirroring the location of the pre-existing natural groundwater seepage zone. In addition to this, quantitative analysis of surface temperatures in the Subdomain B2 seepage zone showed a progressive decline in minimum surface temperature throughout the monitoring period (Figure 13). This sustained decrease reflects the ongoing advection of cooler injected water through hydraulically active fractures.

Discussion

The primary aim of this study was to evaluate the capability of passive and active infrared thermography (IRT) as a non-invasive tool for visualising subsurface heterogeneity and preferential seepage patterns in unsaturated fractured rock masses within an open-pit high wall. The fundamental research contribution lies in providing direct, empirical evidence of flow localisation, time-dependent activation, and advective cooling along hydraulically active discontinuities. By combining ambient thermal monitoring with controlled thermal stimulation (cold-water injection), this approach successfully detected both natural and induced thermal anomalies. These results confirm the effectiveness of infrared thermography (IRT) for identifying seepage zones and provide valuable insights into flow behaviour in fractured rock environments.

Interpretation of passive and active thermal signatures

Passive infrared thermography (IRT) proved to be a reliable method for establishing baseline conditions and detecting natural thermal anomalies associated with groundwater seepage. Under ambient temperatures, the most pronounced thermal signatures appeared in Domain B, where water seepage from the high wall produced cooler surface patterns that matched geotechnical window mapping results (as shown Figure 9). The clear thermal contrast between moist (cooler) groundwater zones and adjacent dry rock highlights the effectiveness of passive IRT as an efficient, non-invasive tool for mapping seepage zones. These findings are consistent with those of Gigli et al. (2014), who observed that moisture zones exhibit distinct, cooler thermal signatures than drier areas on target objects during monitoring, due to evaporative cooling.

To simulate seepage infiltration in fractured rock mass, active infrared thermography was implemented by pumping cold water (~3 °C) into the borehole. This method enabled real-time monitoring of active flow pathways by detecting thermal contrasts between the water and the high wall. Geotechnical domains within the monitored high wall exhibited distinct preferential flow patterns determined by the extent of fracturing and connectivity of discontinuities (refer to Figure 8). In Domain A, where the rock is predominantly massive with low secondary permeability, no thermal contrasts were observed. These thermal results indicate that conditions within this domain were not conducive to rapid fracture controlled seepage. Thus, any minor infiltration that may have occurred was likely limited to matrix flow, progressing at rates insufficient to produce observable cooling anomalies during the monitoring period. In contrast, Domain B, featuring higher fracture density and well-interconnected discontinuities, promoted rapid preferential channelling of water within the high wall. This resulted in markedly stronger, more persistent, and spatially extensive thermal anomalies, reflecting enhanced advective cooling along dominant flow paths.

Furthermore, Domain B was subdivided into Subdomains B1 and B2 for a detailed thermal analysis. In Subdomain B1 (Figure 10), qualitative thermograms effectively identified the natural groundwater discharge zone but were unable to detect additional seepage areas, reflecting the inherent limitations of static thermal imaging under low thermal-contrast conditions. To overcome this, complementary quantitative time-series monitoring was employed, revealing cooling trends indicating subsurface connectivity within this subdomain. In contrast, thermal imaging in Subdomain B2 (Figure 12) revealed the emergence of a new seepage zone. Quantitative surface-temperature analysis further demonstrated a progressive decline in minimum temperatures throughout the monitoring period. Subsequently, reflecting ongoing advection of cooler water flow through hydraulically active fractures within the high wall.

Differences in thermal signatures between Subdomains B1 and B2 highlight the complementary benefits of combining qualitative and quantitative thermal results to improve the interpretation of active IRT data. Qualitative evaluation of thermal images reveals how water moves and localises along preferential flow paths within fractured rock, providing direct insight into fracture flow heterogeneity. This approach captures the initial formation and progressive expansion of cooling anomalies directly linked to active seepage zones, thereby offering important contextual information on flow localisation within the fractured rock mass. This represents a meaningful advance for unsaturated fracture flow as monitoring techniques are often inferred indirectly from geological knowledge and assumed connectivity patterns. While visual interpretation of thermal images may miss early signs of water infiltration, quantitative analysis excels at detecting the onset and precise timing of advective cooling in high walls. It offers superior sensitivity to subtle temperature drops that are frequently masked by environmental noise or too faint to discern visually, especially during the initial phases of water infiltration. Combining both qualitative and quantitative approaches prove valuable under changing environmental conditions, such as unsaturated flow into fractured rock mass.

Flow behaviour in fractured high wall

The observed behaviour provides important insights into unsaturated fracture flow. Subsurface heterogeneity arises from variations in fracture density, connectivity, aperture, roughness, and lithological contacts. These factors govern the development of preferential pathways under transient conditions. In Domain A, massive rock restricts flow to matrix-dominated processes and supports dual domain models that predict limited fracture matrix interaction in low permeability zones. In contrast, Domain B demonstrates rapid channelled advective cooling and delayed secondary seepage, which illustrates flow focusing along connected discontinuities. These findings align with established conceptual models of unsaturated flow in fractured rock. Dual-permeability frameworks describe fractures as the main conduits for rapid preferential flow, while the rock matrix allows for slower storage and imbibition, e.g., Gerke and Van Genuchten (1993) and Berkowitz (2002). This study extends these concepts by providing in situ empirical evidence of preferential pathway in fractured rock mass using infrared thermography.

Infrared thermography (IRT) revealed two distinct seepage zones on the high wall face. The first, a natural seepage zone, was detected during initial passive IRT surveys (Subdomain B1), while the secondary seepage zone emerged in Subdomain B2 during active IRT monitoring. Both seepage zones were located at the contact between quartzitic sandstone and weathered diabase, demonstrating the role of such lithological contacts as high-transmissivity horizons. In addition to this, variability in fracture aperture further controls where seepage zones develop, with larger apertures promoting focused channelling and higher flow rates, while narrower segments and asperities cause capillary bridges, local bottlenecks, and tortuous, pressure-dependent pathways (Berkowitz, 2002). At these contact zones, geometric alignment, bedding plane continuity, and connected fracture networks govern preferential flow and enable rapid pathway activation (Xu et al., 2021; Zimmerman, Paulsny, 2023).

Furthermore, active infrared thermography experiments indicate that seepage in this fractured rock mass is highly sensitive to transient hydraulic gradients. This sensitivity is evidenced by the delayed appearance of a secondary seepage zone, which emerged ~40 minutes after field tests began. The time-dependent delay suggests that fluid flow within the fractured rock mass at the study site is primarily controlled by discontinuity characteristics such as surface roughness, asperity distribution, and thin infills (refer to Table 2). As a result, these characteristics govern fluid pathways, transmissivity, and preferential channelling as highlighted in various studies (Chen et al., 2017; Luo et al., 2022). Moreover, fracture topography also influences seepage migration, as surface roughness may either impede or enhance flow depending on the configuration of discontinuities (Dippenaar, Van Rooy, 2016). Ultimately, seepage zones commonly form along bedding-plane parallel or sub-parallel pathways, shaped by surface morphology and variable wetting resistance under unsaturated conditions.

These observations highlight the limitations of relying on visual inspections or traditional methodologies for assessing fluid flow in fractured rock masses. As highlighted in this study, the principal challenge in managing unsaturated fluid flow in rock engineering is not merely identifying major discontinuity sets, but determining which of these are hydraulically active within specific geotechnical zones. This challenge is especially critical in open-pit environments, where unsaturated fracture flow during infiltration events can cause rapid pore pressure increases along hydraulically active discontinuities. This process reduces effective stress and shear strength, thereby promoting rock slope instability (Li et al., 2024).

Thus, the present study was carried out at a site with a known history of infiltration-induced slope failure, providing key context for unsaturated flow behaviour in fractured high walls. The application of infrared thermography (IRT) as a non-invasive monitoring tool demonstrated its practical utility for identifying zones of preferential seepage. By detecting thermal anomalies indicative of such zones, IRT enabled spatial delineation of areas most susceptible to seepage within the fractured rock mass. This technique offers an advantage over conventional methods, which generally do not provide direct evidence of active flow paths.

Limitations

Despite the proven effectiveness of both passive and active infrared thermography (IRT) in detecting seepage zones within fractured rock masses, several important limitations remain. While the use of a controlled setup, a single quarry bench with one injection source helped reduce experimental variables and enabled clear interpretation of thermal signals, it also restricted the scale of the investigation. Consequently, the findings serve primarily as valuable initial guidance for IRT based seepage visualisation studies. In addition, IRT is highly sensitive to environmental influences such as solar radiation, weather conditions, viewing angles, and variations in rock emissivity. These factors can easily obscure the subtle thermal contrasts required for reliable seepage detection. A further limitation lies in the need for IRT processing techniques. Translating two dimensional thermal images need to be inferred to complex fracture flow paths and subsurface seepage areas in high wall demand advanced post-processing methods. This step not only requires specialised expertise but also entails significant computational resources.

Conclusion

This study has demonstrated infrared thermography (IRT) as a promising, non-invasive method for detecting seepage zones in fractured rock mass. This was achieved by integrating geotechnical characterisation of the quartzitic sandstone intruded by diabase with temperature distribution analysis along the southwestern highwall of the quarry.

Passive IRT under ambient conditions revealed distinct thermal signatures linked to the natural groundwater seepage zone, making it clearly distinguishable from the surrounding rock mass. Complementary active thermography field tests, involving the controlled introduction of colder water, simulated flow dynamics. Domain A exhibited minimal thermal response, which is consistent with low-permeability massive rock. In contrast, Domain B displayed rapid and heterogeneous thermal changes. These changes indicate discontinuity-controlled, unsaturated flow along preferential pathways. Moreover, groundwater and infiltration-induced seepage zones were most evident at the contact between quartzitic sandstone and weathered diabase. This shows that these lithological contacts are the most hydraulically conductive features in the rock mass even during active IRT surveys.

Thus, routine integration of passive and active IRT could enable early detection of thermal anomalies linked to seepage zones in similar fractured environments. Unlike traditional techniques such as borehole monitoring, moisture sensors, or visual inspections, most methods provide only indirect signs of possible flow zones. In contrast, IRT offers direct visualisation of seepage, early anomaly detection, and real-time tracking of evolving subsurface flow processes based on thermal contrasts. These capabilities, often challenging to achieve with conventional methods alone, demonstrate the novelty and practical value of IRT as a monitoring tool. They support proactive geohazard management in open-pit mining environments by enabling early warning of seepage-induced slope instability or uncontrolled groundwater inflow during excavation.

To guide future work, several areas for further study can build on these advancements. Key research directions include:

- ➤ Scale monitoring to full highwall or open-pit levels, with multiple injection points to map flow heterogeneity in complex fracture systems.
- ➤ Develop real-time IRT systems incorporating machine learning for environmental noise reduction and automated anomaly alerting to support geotechnical decision-making.
- ➤ Integrate IRT with complementary tools (e.g., drone-based imaging, photogrammetry) for multi-modal, cost-effective monitoring.
- ➤ Undertake long-term studies across diverse local lithologies, structures, and climatic conditions to establish standardised IRT protocols for seepage detection and risk assessment.

Acknowledgements

The financial support from the National Research Foundation (NRF) through the Thuthuka programme, the Water Research Commission (Project No. C2020/2021-00581), and SRK Consulting, Johannesburg, is gratefully acknowledged.

Author contributions

The following authors contributed to the study conception and design Mampho Maoyi, Prof J Louis van Rooy (Supervisor) and Prof Matthys Dippenaar (Supervisor). Material preparation, data collection and analysis were performed by Mampho Maoyi, Rory Bush (photogrammetry) and Andre Lotriet (Thermographer). The first draft of the manuscript was written by Mampho Maoyi and all authors commented on previous versions of the manuscript.

References

Abdulai, M., Sharifzadeh, M. 2019. Uncertainty and reliability analysis of open pit rock slopes: a critical review of methods of analysis. Geotechnical and Geological Engineering, vol. 37, pp.1223-1247. https://doi.org/10.1007/s10706-018-0680-y

Barton, N., Lien, R., Lunde, J.J.R.M. 1974. Engineering classification of rock masses for the design of tunnel support. Rock mechanics, vol. 6, pp.189-236. https://doi.org/10.1007/BF01239496

Berkowitz, B. 2002. Characterizing flow and transport in fractured geological media: A review. *Advances in water resources*, vol. 25 no. 8-12, pp.861-884.

Bieniawski, Z.T. 1973. Engineering classification of jointed rock masses. Civil Engineering= Siviele Ingenieurswese, vol. 1973, no.12, pp.335-343.

Bieniawski, Z.T. 1989. Engineering rock mass classifications: a complete manual for engineers and geologists in mining, *civil, and petroleum engineering*. John Wiley & Sons.

Chen, Z., Qian, J., Zhan, H., Zhou, Z., Wang, J., Tan, Y. 2017. Effect of roughness on water flow through a synthetic single rough fracture. Environmental earth sciences, vol. 76, no. 4, p.186.

Council for Geoscience. 1978. 1:250 000 Geological Map of 2528 Pretoria. Data Management Portal. Category: Geology. Updated December 2020. https://maps.geoscience.org.za/portal/apps/sites/#/council-for-geoscience-interactive-web-map-1

Dippenaar, M.A., Van Rooy, J.L. 2016. On the cubic law and variably saturated flow through discrete open rough-walled discontinuities. *International Journal of Rock Mechanics and Mining Sciences*, vol. 89, pp.200-211.

Eriksson, P.G., Reczko, B.F.F. 1995. The sedimentary and tectonic setting of the Transvaal Supergroup floor rocks to the Bushveld Complex. *Journal of African Earth Sciences*, vol. 21, no. 4, pp.487-504. https://doi.org/10.1016/0899-5362(95)00111-5

Eriksson, P.G., Altermann, W., Hartzer, F.J., Johnson, M.R., Anhaeusser, C.R., Thomas, R.J. 2006. The Transvaal Supergroup and its precursors. *The Geology of South Africa*, pp.237-260.

Gerke, H.H., Van Genuchten, M.T. 1993. A dual-porosity model for simulating the preferential movement of water and solutes in structured porous media. *Water resources research*, vol. 29, no. 2, pp.305-319.

Gigli, G., Frodella, W., Garfagnoli, F., Morelli, S., Mugnai, F., Menna, F., Casagli, N. 2014. 3-D geomechanical rock mass characterization for the evaluation of rockslide susceptibility scenarios. *Landslides*, vol. 11, pp.131-140. https://doi.org/10.1007/s10346-013-0424-2

Huang, N., Jiang, Y., Liu, R., Li, B., Sugimoto, S. 2019. A novel three-dimensional discrete fracture network model for investigating the role of aperture heterogeneity on fluid flow through fractured rock masses. *International Journal of Rock Mechanics and Mining Sciences*, vol. 116, pp.25-37. https://doi.org/10.1016/j.ijrmms.2019.03.014

International Society for Rock Mechanics. 1978. Suggested Methods for the Quantitative Description of Discontinuities in Rock Masses. Rock Characterisation Testing and Monitoring.

Kaveh Ahangaran, D., Ahangari, K., Eftekhari, M. 2022. Numerical analysis of blast-induced damage in rock slopes. Innovative Infrastructure Solutions, vol. 7, no.1, p.83. https://doi.org/10.1007/s41062-021-00684-w

Laubscher, D.H. 1990. A geomechanics classification system for the rating of rock mass in mine design. *Journal of the Southern African Institute of Mining and Metallurgy*, vol. 90, no.10, pp.257-273. https://doi.org/10.1016/0148-9062(91)90830-F

Li, T., Song, H., Huang, G., Bi, Y., Li, X. 2014. Assessment of groundwater changing trends through the generalized large well method with confined–unconfined flow model in open-pit mine area. Environmental Earth Sciences, vol. 72, pp.4599-4606. https://doi.org/10.1007/s12665-014-3357-8

Li, X., Li, Q., Wang, Y., Liu, W., Hou, D., Zhu, C. 2024. Effect of slope angle on fractured rock masses under combined influence of variable rainfall infiltration and excavation unloading. *Journal of Rock Mechanics and Geotechnical Engineering*, vol. 16, no.10, pp.4154-4176. https://doi.org/10.1016/j.jrmge.2024.08.019

Liu, Q., Zhang, Z., Zhang, B., Mu, W., Zhang, H., Li, Y., Xu, N. 2021. Hydrochemical analysis and identification of open-pit mine water sources: A case study from the Dagushan iron mine in Northeast China. *Scientific Reports*, vo.11, no.1, p.23152.

Lu, Y., Jin, C., Wang, Q., Li, G., Han, T. 2024. Deformation and failure characteristic of open-pit slope subjected to combined effects of mining blasting and rainfall infiltration. *Engineering Geology*, vol. 331, p.107437. https://doi.org/10.1016/j.enggeo.2024.107437

Luo, Y., Zhang, Z., Zhang, L., Xue, K., Long, K. 2022. Influence of fracture roughness and void space morphology on nonlinear fluid flow through rock fractures. *The European Physical Journal Plus*, vol. 137, no.11, p.1288.

Meola, C. 2012. Origin and theory of infrared thermography. *Infrared Thermography Recent Advances and Future Trends, Bentham eBooks*, pp.3-28. https://doi.org/10.2174/978160805143411201010003

Mineo, S., Pappalardo, G. 2021. Rock emissivity measurement for infrared thermography engineering geological applications. *Applied Sciences*, vol.11, no.9, p.3773. https://doi.org/10.3390/app11093773

Mineo, S., Calcaterra, D., Zampelli, S.P., Pappalardo, G. 2015. Application of Infrared Thermography for the survey of intensely jointed rock slopes. *Rendiconti Online della Società Geologica Italiana*, vol.35, pp.212-215. https://doi.org/10.3301/ROL.2015.103

Rosenbom, A.E., Jakobsen, P.R. 2005. Infrared thermography and fracture analysis of preferential flow in chalk. *Vadose Zone Journal*, vol.4, no.2, pp.271-280. https://doi.org/10.2136/vzj2004.0074

Sass, O., Bauer, C., Heil, S., Schnepfleitner, H., Kropf, F., Gaisberger, C. 2023. Infrared thermography monitoring of rock faces–Potential and pitfalls. *Geomorphology*, vol. 439, p.108837. https://doi.org/10.1016/j.geomorph.2023.108837

Silva, J., Worsey, T., Lusk, B. 2019. Practical assessment of rock damage due to blasting. *International Journal of Mining Science and Technology*, vol.29, no.3, pp.379-385. https://doi.org/10.1016/j.ijmst.2018.11.003

Teza, G., Marcato, G., Castelli, E., Galgaro, A. 2012. IRTROCK: A MATLAB toolbox for contactless recognition of surface and shallow weakness of a rock cliff by infrared thermography. *Computers & Geosciences*, vol. 45, pp.109-118. https://doi.org/10.1016/j.cageo.2011.10.022

Usamentiaga, R., Venegas, P., Guerediaga, J., Vega, L., Molleda, J., Bulnes, F.G. 2014. Infrared thermography for temperature measurement and non-destructive testing. Sensors, vol.14, no.7, pp.12305-12348. https://doi.org/10.3390/s140712305

Vollmer, M., Möllmann, K.P. 2018. Infrared thermal imaging: fundamentals, research and applications. John Wiley & Sons.

Wu, J.H., Lin, H.M., Lee, D.H., Fang, S.C. 2005. Integrity assessment of rock mass behind the shotcreted slope using thermography. *Engineering geology*, vol. 80, no.1-2, pp.164-173.

Xu, P., Yang, R., Zuo, J., Ding, C., Chen, C., Guo, Y., Fang, S., Zhang, Y. 2022. Research progress of the fundamental theory and technology of rock blasting. *International Journal of Minerals, Metallurgy and Materials*, vol.29, no.4, pp.705-716. https://doi.org/10.1007/s12613-022-2464-x

Xu, Y., Liao, X., Li, J., Chen, L., Li, L. 2021. The Effects of Water Content and Dry–Wet Cycles of Weak-Interlayer Soil on Stability of Clastic Rock Slope. *Geotechnical and Geological Engineering*, vol. 39, pp.3753-3760. https://doi.org/10.1007/s10706-021-01722-1

Yeh, C.H., Dong, J.J., Khoshnevisan, S., Juang, C.H., Huang, W.C., Lu, Y.C. 2021. The role of the geological uncertainty in a geotechnical design–A retrospective view of Freeway No. 3 Landslide in Northern Taiwan. *Engineering Geology,* vol.291, pp.106233. https:/doi.org/10.1016/j.enggeo.2021.106233

Zangerl, C., Koppensteiner, M., Strauhal, T. 2022. Semiautomated statistical discontinuity analyses from scanline data of fractured rock masses. *Applied Sciences*, vol.12, no.19, pp.9622.

Zhang, Q., Huang, X., Zhu, H., Li, J. 2019. Quantitative assessments of the correlations between rock mass rating (RMR) and geological strength index (GSI). Tunnelling and Underground Space Technology, vol.83, pp.73-81. https://doi.org/10.1016/j.tust.2018.09.015

Zhang, X., Ma, F., Yin, S., Wallace, C.D., Soltanian, M.R., Dai, Z., Ritzi, R.W., Ma, Z., Zhan, C., Lü, X. 2021. Application of upscaling methods for fluid flow and mass transport in multi-scale heterogeneous media: A critical review. Applied energy, 303, p.117603. https://doi.org/10.1016/j.apenergy.2021.117603

Zhao, L., Ren, T., Wang, N. 2017. Groundwater impact of open cut coal mine and an assessment methodology: A case study in NSW. *International Journal of Mining Science and Technology*, vol.27, no.5, pp.861-866. https://doi.org/10.1016/j.ijmst.2017.07.008

Zimmerman, R.W., Paluszny, A. 2023. Fluid flow in fractured rocks. John Wiley & Sons. ◆

SAMCODES
SAMCODES STANDARDS COMMITTEE
THE SOUTH AFRICAN MINERAL REPORTING CODES

The Focus for SAMCODES in Q2 2026

During Q2 2026, SAMCODES continued to focus on the planned update of the SAMREC Code, including preparation for industry consultation and alignment with evolving international reporting standards. Work also progressed on the integration of ESG guidance, education and training initiatives, and broader stakeholder engagement.

The SSC also advanced its promotion and sponsorship activities, while preparing for upcoming CRIRSCO, SAMREC/SAMVAL and other SAMCODES-related events.

LinkedIn

The SAMCODES LinkedIn page continues to be used to share current developments, industry updates and recognition of contributors. Appreciation posts are being prepared for long-serving SSC contributors, including Annalie de Bruyn and Rob Ingram. https://www.linkedin.com/company/samcodessa/

SAMCODES App

- The App continues to provide a convenient platform for accessing current SAMCODES information.
- The updated SAMCODES App User Guide is being maintained on the SAMCODES website, with refreshed guidance to support users. Committee quiz questions are also being developed, with previous examples being circulated to help avoid duplication.

Committee updates

SAMREC THE SOUTH AFRICAN CODE FOR THE REPORTING OF EXPLORATION RESULTS, MINERAL RESOURCES AND MINERAL RESERVES	The SAMREC Committee is preparing the pre-update survey and progressing the Code rewrite. Follow-up engagement with SAMESG is planned to resolve outstanding ESG Guideline matters.
SAMVAL THE SOUTH AFRICAN CODE FOR THE REPORTING OF MINERAL ASSET VALUATION	Planning continues for a SAMREC and SAMVAL Advanced Workshop, with further details to be confirmed.
SAMOG THE SOUTH AFRICAN CODE FOR THE REPORTING OF OIL AND GAS RESOURCES	The proposed SAMOG Governance and Mandate review submitted by Andy Clay is under review.
	Engagement between the SAMREC and SAMESG Committees is continuing to address outstanding matters relating to the SAMESG Guideline and its integration with the forthcoming SAMREC Code update. A follow-up meeting between the committees is planned to resolve outstanding issues.
SAMCODES SAMCODES STANDARDS COMMITTEE THE SOUTH AFRICAN MINERAL REPORTING CODES	Annalie de Bruyn retired from the JSE in July 2026. Zakaria Rashid will succeed her as the JSE representative on the SSC. Rob Ingram has retired as Chair of the JSE Readers Panel, with Andy McDonald succeeding him.

Training and Development

Compliance and Reporting Rules Course, MINN7052A was offered from 20 - 24 July 2026 through Wits University and coordinated by Dr Tania Marshall. The aim of the course is to upskill and create awareness on compliance requirements and Mineral Reporting Codes.

International Liaison

UNECE Resource Management Week 2026 was held from 27 April to 1 May 2026, highlighting the importance of UNFC classifications and resource management frameworks.

The AMREC-PARC-UNFC Workshop was held on 12-13 May 2026, with Tania Marshall invited to present on SAMREC. The next CRIRSCO AGM is scheduled for 7-11 September 2026 in Türkiye and will incorporate an IMVAL event.

The SSC is also progressing engagement with key South African stakeholders, including the Council for Geoscience and Minerals Council South Africa, with meetings to be scheduled.

Management Update

The SSC Annual Report covering June 2025 to May 2026 has been completed. The SSC is also reviewing its Governance and Mandate documentation, confirming member representation, and preparing the October 2026 update to the GSSA and SAIMM. Joseph Mainama continues as SSC Chair, supported by Jacques Nel as Deputy Chairperson.